This is the peer reviewed version of the following article: Giuffrida, A., Moioli, S., Romano, M.C., Lozza, G., Lignite-fired air-blown IGCC systems with pre-combustion CO2 capture, International Journal of Energy Research, 2016, which has been published in final form at https://doi.org/10.1002/er.3488. This article may be used for non-commercial purposes in accordance with Wiley Terms and Conditions for Use of Self-Archived Versions.

Lignite-fired air-blown IGCC systems with pre-combustion CO2 capture

Antonio Giuffrida1*†, Stefania Moioli[2], Matteo C. Romano[1] and Giovanni Lozza[1]

1Dipartimento di Energia, Politecnico di Milano, Via Raffaele Lambruschini 4, Milano, 20156, Italy
2Dipartimento di Chimica, Materiali e Ingegneria Chimica "G. Natta", Politecnico di Milano, Piazza Leonardo da Vinci 32, Milano, 20133, Italy

SUMMARY

Detailed analyses based on mass and energy balances of lignite-fired air-blown gasification-based combined cycles with CO_2 pre-combustion capture are presented and discussed in this work. The thermodynamic assessment is carried out with a proprietary code integrated with Aspen Plus® to carefully simulate the selective removal of both H_2S and CO_2 in the acid gas removal station. The work focuses on power plants with two combustion turbines, with lower and higher turbine inlet temperatures, respectively, as topping cycle. A high-moisture lignite, partially dried before feeding the air-blown gasification system, is used as fuel input. Because the raw lignite presents a very low amount of sulfur, a particular technique consisting of an acid gas recycle to the absorber, is adopted to fulfill the requirements related to the presence of H_2S in the stream to the Claus plant and in the CO_2-rich stream to storage.

Despite the operation of the H_2S removal section representing a significant issue, the impact on the performance of the power plant is limited. The calculations show that a significant lignite pre-drying is necessary to achieve higher efficiency in case of CO_2 capture. In particular, considering a wide range (10–30 wt.%) of residual moisture in the dried lignite, higher heating value (HHV) efficiency presents a decreasing trend, with maximum values of 35.15% and 37.12% depending on the type of the combustion turbine, even though the higher the residual moisture in the dried coal, the lower the extraction of steam from the heat recovery steam cycle. On the other hand, introducing the specific primary energy consumption for CO_2 avoided (SPECCA) as a measure of the energy cost related to CO_2 capture, lower values were predicted when gasifying dried lignite with higher residual moisture content. In particular, a SPECCA value as low as 2.69 MJ/kg_{CO2} was calculated when gasifying lignite with the highest (30 wt.%) residual moisture content in a power plant with the advanced combustion turbine.

Ultimately, focusing on the power plants with the advanced combustion turbine, air-blown gasification of lignite brings about a reduction in HHV efficiency equal to almost 1.5 to 2.8 percentage points, depending on the residual moisture in the dried lignite, if compared with similar cases where bituminous coal is used as fuel input.

KEY WORDS: air-blown; CCS; drying; IGCC; lignite; MDEA; SPECCA; TIT

1. INTRODUCTION

Coal is likely to be one of the main sources of primary energy for the next several decades, as fuel input in power plants for electricity generation, based on its relatively low price compared with other fossil fuels and the largest proven resources in the world. In particular, low rank coals, including sub-bituminous coal as well as lignite or brown coal, account for more than 50% of the world coal reserves. However, their use is limited because of low heating value and hazardous spontaneous combustion properties.

Because of the challenges of global warming and environmental pollution from burning coal, a growing interest has been oriented in recent years to the development of clean coal technologies [1] that cover flue gas treatments, high efficiency combustion, gasification, and carbon capture and storage (CCS). In particular, coal gasification is a flexible and reliable technology that can turn a variety of feedstocks [2] into high-value products [3], as well as

Received 24 March 2015;
Revised 26 November 2015;
Accepted 3 December 2015

Correspondence
† *Antonio Giuffrida, Politecnico di Milano - Dipartimento di Energia, Via Raffaele Lambruschini 4, 20156 Milano, Italy.
E-mail: antonio.giuffrida@polimi.it

help to reduce dependence on oil and natural gas [4]. Coal gasification is the core of an integrated gasification combined cycle (IGCC). Although most of the R&D and demonstration projects on large-scale IGCCs are based on oxygen-blown gasification systems, air-blown gasification should also be considered as an option because of the economic advantage related to the much smaller air separation unit [5,6] and the potentially higher IGCC efficiency [7]. A significant activity on air-blown coal gasification has been conducted during the last years by Mitsubishi Heavy Industries (MHI) in Japan, where the 1700 tpd-250 MW_{el} demonstration plant in Nakoso was started up in 2007 [8], after preliminary research activities on lab-scale gasifiers and pilot plants. On the basis of public information from MHI, a complete IGCC power plant was formerly modeled by the authors [7], after reproducing the mass and energy balances of a large-scale MHI-type air-blown gasifier. Its performance was compared with the one of an IGCC based on an oxygen-blown Shell-type gasifier, calculated with coherent assumptions. As a significant outcome, the net efficiency resulted 1.5 percentage points higher than the one characterizing the reference oxygen-blown IGCC. Further studies on air-blown IGCC systems were carried out as well, paying attention to solutions based on hot fuel gas clean-up technology [9] and to pre-combustion and post-combustion CO_2 capture [10–13].

Especially with lignite as fuel input in power plants, having high specific CO_2 emissions because of low conversion efficiencies, CCS would be highly beneficial from an environmental point of view. Several technologies have been investigated for pre-combustion IGCC power plants fired with low rank coals. Physical scrubbing with the Rectisol® process was investigated by Klimantos *et al.* [14] and by Gräbner *et al.* [15], with efficiency losses equal to 10.2 percentage points (on a lower heating value (LHV) basis) for 74% of CO_2 avoided [15]. A report by the National Energy Technology Laboratory of the U.S. Department of Energy investigated IGCC cases with different gasification technologies [16]: achieving a CO_2 capture of 90% with a Selexol™ process, higher heating value (HHV) efficiency reduces from 41.8% to 31.7% and from 37.6% to 30% in case of a Shell-type and a Siemens-type gasification system, respectively. Mondol *et al.* [17] proposed a process based on the Absorption Enhanced Reforming reaction that combines steam gasification of lignite with the high-temperature CO_2 removal by using high-temperature efficient sorbent materials, namely CaO. The results showed that the proposed CO_2 capture plants efficiencies were 18.5–21% higher than the conventional IGCC CO_2 capture plant [17]. For the proposed plants, the CO_2 capture efficiencies were found to be within 95.8–97%. Pre-combustion CCS via porous ceramic membranes in lignite-fired IGCC power plants has been recently investigated by Maas and Scherer [18]. Focusing on four different IGCC cases with capture rates over 97.5%, the achievable efficiency losses lay between 6.8 and 9.4 percentage points. As a matter of fact, all these investigated IGCC cases are based on the oxygen-blown technology, so literature is lacking in studies of CCS in air-blown IGCC systems.

Here, detailed analyses based on mass and energy balances of lignite-fired air-blown IGCC systems with CO_2 pre-combustion capture are presented and discussed, after having described a complete IGCC system. Particular attention in modeling and simulation is paid to the acid gas removal (AGR) station, as regards both H_2S and CO_2 removal. A methyldiethanolamine (MDEA)-based process is considered, instead of other capture technologies based on physical absorption (e.g., Selexol™ process), justified by the limited CO_2 partial pressure in the coal-derived gas because of the significant amount of nitrogen. It is however recognized by the authors that both physical and chemical absorption processes may be suitable for this application, considering the CO_2 partial pressures in the raw syngas. A comparative analysis between the two options, which would be necessary to define the optimal process and should include an economic analysis, is however beyond the scope of this work.

2. DESCRIPTION OF THE IGCC

The layout of the air-blown IGCC systems considered in this work is based on the one already investigated by the authors [7]. Each power plant consists of two gasification trains and two combustion turbines (CTs) with two heat recovery steam generators (HRSGs), which share the same steam turbine.

2.1. The gasification station

Referring to the IGCC layout in Figure 1, dried lignite (2) is loaded with a dry lock hopper system by means of a fraction of the CO_2 captured in the AGR station and recycled back (3), so that the air separation unit, necessary in the power plant with no CO_2 capture to produce the pure nitrogen for coal loading, is not employed here [19]. A system based on the WTA (German acronym for 'fluidized bed dryer with integrated waste heat recovery') process, as proposed by RWE Power AG, is used for lignite pre-drying [19]. As schematized in Figure 2, the heat necessary for moisture heating and evaporation is mainly provided by pressurized steam from the previous charge drying, which condenses in the heat exchanger immersed in the fluidized bed dryer [20].

The air-blown coal gasification system, as developed by MHI [5,8], is a water-wall, two-stage entrained flow gasifier. Such a configuration allows for a carbon conversion of the order of 99.9% [5] in the bottoming stage, that is, the combustor, where coal and recycled char are burnt at high temperature (about 1900°C) with high air-to-coal ratio. In the topping stage, high-temperature syngas is chemically quenched and experiences a temperature drop of about 700°C. Because of the lower

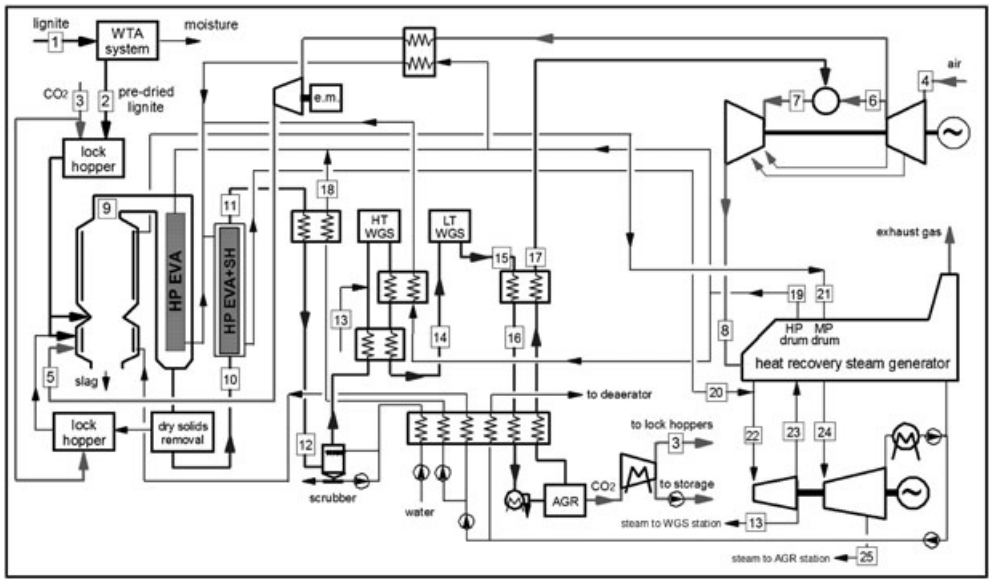

Figure 1. Layout of the lignite-fired air-blown IGCC system with pre-combustion CO_2 capture.

temperature, the coal-derived gas exiting the gasifier contains a certain amount of unconverted carbon, which is collected by a cyclone and recycled back to the combustor stage. As shown in Figure 1, the air for coal gasification is extracted from the CT compressor outlet, partly cooled down to about 350°C by producing high pressure (HP) steam and finally boosted to the gasification system. The coal-derived gas exiting the gasifier is cooled down to about 350°C (11) by producing HP super-heated steam and is then further cooled down (12), before scrubbing, by economization of HP water. A sour water–gas shift (WGS) station, with two reactors and two heat exchangers, is present after the scrubber. In detail, the syngas exiting the scrubber is first pre-heated in a recuperative gas–gas heat exchanger and then mixed with medium pressure (MP) steam (13), extracted from the heat recovery steam cycle, before entering the first WGS reactor. The shifted syngas exiting the HT-WGS reactor at temperature slightly less than 500°C is first cooled down to about 350°C by producing HP steam and used as the hot stream in the regenerative gas–gas heat exchanger to pre-heat the syngas exiting the scrubber. Then, the shifted syngas at 210°C (14) enters the LT-WGS reactor to complete the conversion of CO into CO_2. An overall CO conversion higher than 97% is obtained in the WGS station, and more than 95% of the total carbon in the shifted syngas is finally present as CO_2. The shifted syngas exiting the LT-WGS reactor is then cooled down to 150°C (16) by heating the H_2-rich stream fuelling the CT. It is further cooled down

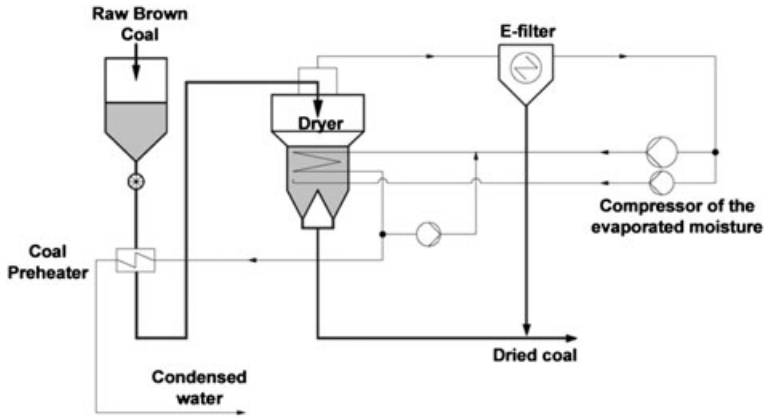

Figure 2. Schematic of the high-moisture coal drying system based on the WTA process.

to near-ambient temperature for AGR, releasing heat for pre-heating the clean syngas from the AGR station and water for the steam cycle and for syngas scrubbing.

2.2. The AGR station

Acid gases removal is carried out by means of a MDEA-based process. Here, H_2S and CO_2 are selectively removed and sent to a Claus unit for sulfur production and to permanent storage, respectively. A selective absorption must be performed in order to satisfy the specifications for the H_2S content (limited to less than 200 ppm) in the CO_2-rich stream to be stored [21].

The AGR station is divided into two plants: one for H_2S absorption and another one for CO_2 absorption (no less than 95% of the CO_2 in the syngas entering the AGR station). Figures 3 and 4 show the schematizations of these purification plants, studied to satisfy the specifications without exceeding in energy requirement, in particular in the regeneration units. These ones are the most energy demanding components in the AGR station [22,23], as the steam needed to heat the reboiler must provide sufficient energy for the endothermic acid gas desorption and generate a vapor stream working as stripping agent along the distillation column [24].

Looking at Figure 3, the stream sent to the AGR station is mixed with two compressed recycle streams, *RECYCLE* and *CLAUSREC*, before entering the first absorption column, which selectively removes H_2S by means of an aqueous diluted amine solution. The solvent, exiting the bottom of the absorption column and rich in H_2S, is regenerated by flash and distillation, studied for energy saving. *FLASH* helps in separating part of the absorbed CO_2 by simply lowering the pressure of the system down to 1 bar, without additional energy supply. In particular, the amount of CO_2 in the *FLASHVAP* stream is very high (85–90% on a molar basis) compared with the one of H_2S, which largely remains in the liquid phase and exits in *H2SPROD* in higher concentration than the one that would be found without the flash unit. Stream *FLASHVAP* also contains the absorbed H_2 (N_2 and water also), which is not lost in this section, but recovered and mixed to the H_2S-free syngas sent to the CO_2 removal section. A heat exchanger (*CROSS*) is present to recover most of the heat supplied at the reboiler of the distillation column and to simultaneously feed the rich amine solution to *REGH2S* at higher temperature. The gaseous stream from the regeneration unit is split into two streams: *H2SPROD* to the Claus unit for sulfur recovery and *RECYCLE* recycled to the absorption section. *CLAUSREC* is a stream containing part of H_2S (4% of the flow rate absorbed from the sour syngas, corresponding to a 96% sulfur recovery efficiency in the Claus plant) and all the CO_2 of stream *H2SPROD* (supposed non-reacted in the Claus unit). The Claus unit is not simulated in this work, but it is considered in order to determine the characteristics of the H_2S-rich stream *H2SPROD* exiting the regeneration column and of the *RECYCLE* stream. In particular, no net steam output is assumed to be obtained in the sulfur recovery unit; that is, the steam raised by H_2S combustion in the Claus plant is supposed to balance the heat required to keep the sulfur molten and to regenerate the SCOT solvent. The gaseous streams exiting the absorption column (*GASOUT1*) and the flash vessel (*FLASHVAP*) are sent to the next plant, as shown in Figure 4.

The CO_2 removal unit is schematized in Figure 4 and consists of two parallel absorption columns with one regeneration column. Both the gaseous feed (*TOCO2ABS*) and the liquid solvent (*LEANPUMP*) are split into two identical streams before entering the columns *ABSCO21* and *ABSCO22*, where most of the CO_2 is absorbed. The rich amine solutions exiting *ABSCO21* and *ABSCO22* are mixed and sent to a single distillation column (*REGCO21*) for regeneration. The lean amine solution, characterized by a low CO_2 content (about $2.7 \cdot 10^{-3}$ on a molar basis) and a very low H_2S content (about 10^{-5} on a molar basis), is pumped to the two absorption columns after passing through a heat exchanger (*CROSS1*) for pre-heating the rich amine solution.

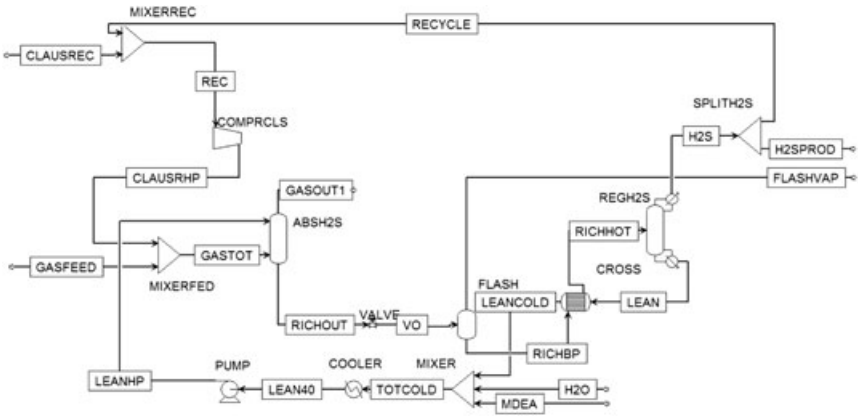

Figure 3. Schematic layout of the H_2S removal unit.

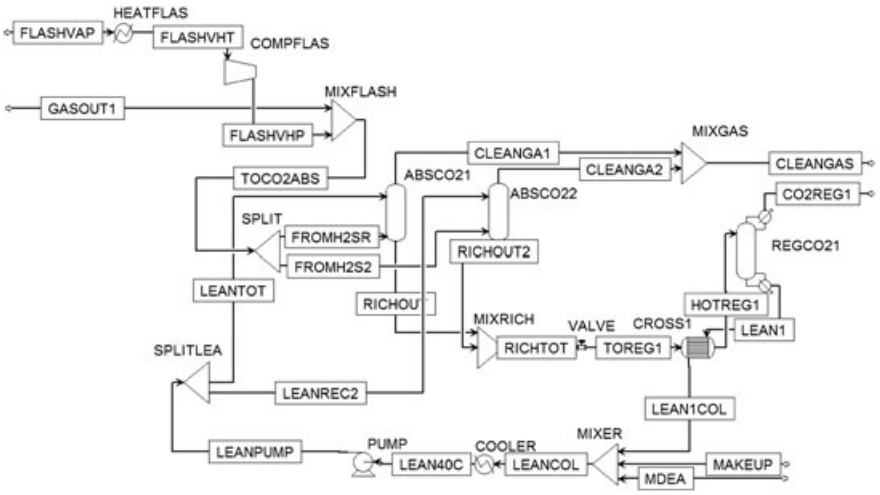

Figure 4. Schematic layout of the CO_2 removal unit.

The stream *CO2REG1* is finally sent to a compression station with five intercooled stages and further split into two streams: one recycled back to the gasification station for coal loading and another pumped to permanent storage.

2.3. The power station

The clean syngas exiting the AGR station is heated up to about 230°C (17) in recuperative heat exchangers before fuelling the CT at the topping cycle of the power station. Two CT technologies have been considered in this work. In particular, the two technologies differ in the turbine inlet temperature (TIT; 1305 vs. 1360°C) and in the required fuel overpressure with respect to the air delivered by the CT compressor. Thus, the CT technology also affects the operating pressure of the gasifier and the syngas cooling and treating stations, as well as the electric consumptions of the air booster, as better detailed hereafter.

The CT exhaust heat is recovered in a two pressure level steam cycle with reheat, where the HP level is always fixed to 144 bar and the MP level is fixed to 40 or 36 bar, depending on the CT technology. This difference in the MP level is selected in order to match the pressure required at the WGS station, which depends on the gasifier pressure, because the steam for the WGS process is assumed to be always extracted from the HP cylinder outlet.

It is worth highlighting that the contribution of syngas cooling to the total steam cycle heat input is really significant for this IGCC with CO_2 capture, owing to (i) the huge presence of nitrogen in the syngas exiting the gasifier, (ii) the increased syngas flow rate with respect to the case with no CO_2 capture [19], (iii) the exothermic WGS reaction, and (iv) the increased syngas flow rate due to the injection of warm steam upstream of the WGS station. Another slight contribution to the steam cycle comes from the gasification air cooling before its boosting.

3. SIMULATION ENVIRONMENTS, ASSUMPTIONS, AND CONSIDERATIONS

The thermodynamic models of the power plants assessed and discussed in the next paragraph were implemented in the proprietary code GS, integrated with the commercial code Aspen Plus®.

3.1. Simulations of gasification and power stations

Mass and energy balances of the previously presented IGCC system were carried out with the simulation code GS [25], which is a proprietary simulation tool originally designed for research purposes at the Department of Energy of Politecnico di Milano to calculate gas–steam cycles and progressively improved to calculate more complex systems. It has proved to yield highly accurate results in estimating the performance of CTs and combined cycles [26] and has been successfully used to calculate mass and energy balances of a variety of power plant configurations, including gasification processes and other chemical reactors [27,28]. The main features of the code include the following: (i) the capability of reproducing very complex plant schemes by assembling basic modules, such as turbine, compressor, combustor, steam section, chemical reactor, heat exchanger, and others; (ii) the use of built-in correlations for efficiency prediction of turbomachinery (gas and steam turbine stages and compressors), as a function of their operating conditions; (iii) the use of built-in correlations for predicting gas turbine cooling flows; and (iv) the capability of calculating chemical equilibrium by Gibbs free energy minimization. Once the system to be calculated is defined as an ensemble of components, mass and energy balances of each component are calculated iteratively,

until the conditions at all interconnections converge toward stable values.

Table A.1 in the Appendix reports the main assumptions for the simulation of the gasification station, distinguishing the two CT technologies (A and B, respectively) considered in this work. Table A.2 details the assumptions for the simulation of the CT performance with reference to the two CT technologies, as suggested by the European Benchmarking Task Force [21]. As regards further details about the assumptions for the calculations of the heat recovery steam cycle (pressure levels in the HRSG were previously reported), reference to other papers [10,19] is made, for the sake of brevity. It is worth to underline that different gasification pressures for cases A and B result from the pressure losses through the various components in the gasification station as well as from the pressure loss at the CT fuel valve.

Table I details the characteristics of the lignite [29] used as fuel for the IGCC systems. Cases with different levels of lignite pre-drying were analyzed. In the following, each simulated case is characterized by a letter (A or B) and by a number (10, 20, 30), where A and B refer to the specific CT at the topping cycle, as anticipated, while numbers indicate the residual moisture content (wt.%) in the dried lignite. Thus, the size of the IGCC system is determined by assuming that the mass flow rate exiting the CT is to be kept at a determined design value (665 kg/s). As regards the energy consumption of the drying system, it is worth to remind that the operation conditions of the process strongly depend on solid–water interactions. Based on previous calculations [19], Figure 5 shows the specific compression work in a WTA-type drying system, significantly affected by the temperature of the condensed moisture (60°C in this work) exiting the drying system.

3.2. Simulation of AGR

The commercial simulator ASPEN Plus® was used as a basis for simulations of the AGR units, because of its capability of being user customized. A reliable model for both thermodynamics and mass transfer with reactions is fundamental for a correct design of the process [30]. As for thermodynamics, vapor–liquid equilibrium is influenced by the chemical reactions occurring in the liquid phase and involving the presence of ionic species. The high non-ideality of the system was described by means of the Electrolyte-NRTL model [31–34], with *ad hoc* parameters [35,36], regressed on the basis of experimental data. As for mass transfer with reactions, the simulation of the absorption and regeneration columns was performed with a rate-based approach, taking the real phenomena occurring on a tray or section packed height into account. ASPEN Plus® by default uses film theory [37], which is found in literature not appropriate for the description of these systems [38–45], because film theory considers a simple representation of mass transfer in the boundary layer, assuming that mass transfer occurs across a stagnant film of given thickness. Detailed studies showed that a 'more complicated model of mass transfer is required to accurately describe diffusion of species' for amine treating systems [46]. Thus, another model, based on the Eddy Diffusivity theory [47] and on the Interfacial Pseudo First Order assumption, was considered and implemented into ASPEN Plus® by means of an external subroutine, as previously applied to different amine scrubbing systems [48–50], for the description of the absorption column. The method was previously verified by comparison with experimental data of temperature and CO_2 mole fraction profiles along the absorption column of a pilot plant [51] and of two industrial plants [52,53].

Table A.3 reports the main characteristics of both the absorption and regeneration columns simulated in this work as concerns the AGR station.

Table I. Lignite characteristics.

Ultimate analysis, wt.% (d.b.)	
Carbon/hydrogen/nitrogen/sulfur/oxygen	66.7/4.7/0.6/0.3/26
Ash	1.7
HHV, MJ/kg (d.b.)	25.9
LHV, MJ/kg (d.b.)	24.87
Moisture, wt.% (a.r.)	65
HHV, MJ/kg (a.r.)	9.07
LHV, MJ/kg (a.r.)	7.12

3.2.1. H_2S removal

Considering that the H_2S-to-CO_2 ratio in the gas entering the AGR station is very low, a diluted amine solvent was used in order to satisfy the desired specifications and to guarantee an acceptable liquid-to-gas ratio. Generally, amines are used in water solutions with concentrations ranging from approximately 10 to 65 wt.% [54,55]. The

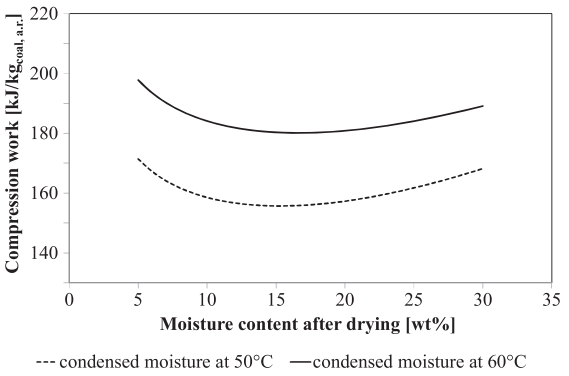

Figure 5. Compression duty for lignite drying as a function of the residual moisture content at two temperatures of the condensed water exiting the drying system.

H_2S-to-CO_2 ratio in the gas entering the AGR station under study is very low, so a diluted amine solvent was considered to be the optimal solution in order to satisfy the desired specifications and to guarantee an acceptable liquid-to-gas ratio. A low MDEA concentration of 10 wt.% has been already considered by other researchers [56,57] and has been chosen in this work because it helps in increasing the liquid flow rate and in maintaining a low residence time. A check of the possible corrosivity of the solution has been carried out. According to the technical literature [58], the corrosion rates in amine solutions are lower than those in water, and for very low MDEA concentrations, the corrosion products could be different than those obtained in high concentrated solutions. However, this would occur for concentrations of about 1 wt.%, much lower than 10 wt.%. In particular, on the basis of detailed experimental data [58], it can be inferred that corrosion effects when using a 10 wt.% MDEA solution are similar to those obtained with more concentrated solutions, so there would not be problems of corrosion of carbon steel [59]. In particular, simulations of the H_2S removal unit without the presence of the recycle stream *RECYCLE* in Figure 3 showed that the gas flowing out of the H_2S stripper was not rich enough in H_2S to fulfill the specifications for feeding the Claus plant (here assuming a minimum H_2S content in the acid gas of 20 vol.%), even considering a wide range of amine solvent flow rates. By recycling part of the gaseous stream exiting the stripping column to the absorption section, the amount of H_2S entering the absorber increases as well as the amount of CO_2 fed to the same column, this last having little effect on the overall CO_2 mass flow rate. As a consequence, the H_2S-to-CO_2 ratio increases: by considering in the *SPLITH2S* unit a split factor equal to 0.5, the molar flow rate of stream *RECYCLE* is the same of stream *H2SPROD*, and the ratio between the amount of H_2S and the one of CO_2 is roughly doubled if compared with the one of the scheme with no recycle.

3.2.2. CO_2 removal

Two parallel absorption columns were considered in the CO_2 removal unit schematized in Figure 4. This configuration was chosen for the cases characterized by lower pressure (24.1 bar, as reported in the Table II), in order to perform the desired CO_2 removal also in the case of a lower driving force. The same cases (B10 to B30) are characterized also by higher CO_2 mass flow rates to be removed, so they would require a higher solvent circulation rate.

Simulations showed that simply increasing the amount of the circulating amine solvent is not favorable for this particular system. The layout proposed in Figure 4, with two parallel absorption columns that treat half the gas flow rate entering the CO_2 absorption section, makes the plant achieve the desired CO_2 removal. As for the cases at higher pressure, even though a single absorption column scheme could have been used [13], the same layout was adopted, in order to guarantee the required specifications without changing the overall structure of the system.

The CO_2 removal unit is the most important section of the AGR station in terms of height of columns, total amine flow rate (ranging from 730 kg/s for case A10 to 1098 kg/s for case B30), and energy consumption. In particular, the reboiler duty necessary in this section is very significant if compared with the one required in the H_2S removal section, as reported in the following.

3.3. Simulation of CO_2 compression

The Peng–Robinson (PR) equation of state was used for the simulation of the CO_2 compression station in ASPEN Plus® [10]. While other models may be more suitable for the calculation of CO_2 mixtures and in the presence of water at HP [60], the PR equation of state is used in this case because of the absence of non-condensable gases and the complete water removal by adsorption at around 15 bar.

Based on an intercooled compression through five stages from 1 to 80 bar (calculated assuming 85% of isentropic efficiency, 94% of mechanical-electric efficiency, and 30°C of intercooling temperatures) with intermediate water adsorption and next liquid CO_2 pumping up to 110 bar, a total specific work equal to 343.8 kJ/kg_{CO2} was calculated, including auxiliary consumptions for heat rejection to the environment in intercoolers.

4. RESULTS AND DISCUSSION

The results of the IGCC and the AGR calculations are here reported and discussed with reference to power balances and main stream characteristics.

Attention is paid first to the details of the coal-derived gas at the AGR station inlet, as reported in Table II where the higher amount of moisture in the lignite clearly causes a reduction in syngas quality. This is due to the higher advancement of the oxidation reactions in the gasifier, calling for an increasing air-to-coal ratio in order to obtain the selected gasification temperature with a feedstock with a higher moisture content. As a result, N_2 concentration increases, while H_2 decreases when considering higher residual moisture, so that higher fuel mass flow rate will be necessary at the CT inlet for a specified firing temperature. Such a deterioration in syngas quality is better pointed out by the cold gas efficiency (CGE)

$$\mathrm{CGE} = \frac{G_{\mathrm{syngas}} \cdot \mathrm{LHV}_{\mathrm{syngas}}}{G_{\mathrm{coal,a.d.}} \cdot \mathrm{LHV}_{\mathrm{coal,a.d.}}} \quad (1)$$

focusing on the dried coal to carbon-free syngas conversion obtained in the gasification island (streams 2 and 17,

Table II. Details of the coal-derived gas at the AGR station inlet (after moisture condensation).

	A10	A20	A30	B10	B20	B30
Temperature, °C				35		
Pressure, bar		29.3			24.1	
Flow rate, kg/s	220	239.8	269.3	246.6	269.4	303.4
Composition, vol%						
Ar	0.50	0.52	0.55	0.50	0.53	0.56
CH_4	0.46	0.51	0.57	0.46	0.51	0.56
CO	0.90	0.86	0.81	0.86	0.82	0.76
CO_2	27.13	27.09	27.04	27.03	27.00	26.94
H_2	29.06	27.09	24.60	28.51	26.53	24.02
H_2O	0.19	0.19	0.19	0.23	0.23	0.23
H_2S	0.04	0.04	0.04	0.04	0.04	0.04
N_2	41.72	43.69	46.20	42.36	44.36	46.89

respectively, in Figure 1). Because of the WGS reaction prior to the AGR, this figure is clearly lower than the one characteristic of the reference IGCC systems without CO_2 capture, as reported in Table III, along with other results, revised because of different assumptions for the CT calculations [19].

Looking at Table IV, power balances and overall results of six IGCC systems are reported. The electric efficiency, calculated as the ratio between the net power output and the lignite thermal input, is introduced as a figure of merit, with reference to both the lignite entering the drying system and the dried lignite to the gasifier.

Focusing on the LHV efficiency calculated in compliance with the dried lignite, IGCC systems based on the established CT technology (cases A10 to A30) present approximately the same efficiency (always around 37%), while a slight reduction can be appreciated for case B30 with respect to the other cases using the advanced CT technology (38.84 vs. 39.08%). This result demonstrates a comparable thermodynamic efficiency of the process downstream the lignite drying system for the cases with CO_2 capture. This result differs from what is obtained for the cases without CO_2 capture [19], where a decreasing trend is always observed for this figure when the residual moisture increases (Table III). In the cases with CO_2 capture, the reduced CGE at high-moisture contents is balanced by the lower steam flow rate extracted from the turbine to achieve the target steam-to-CO ratio at the WGS reactor inlet, because a higher initial steam-to-CO ratio is present in the raw syngas in case of gasification of a fuel with higher moisture.

When referring to the LHV of the as-received lignite, IGCC efficiency always decreases when the residual moisture increases. On the whole, net efficiency values higher than the ones calculated for IGCCs fired with bituminous coals [7] can be appreciated and justified according to the actual ratio between HHV and LHV of the as-received lignite reported in Table I.

Conversely, the drying process does not affect the HHV of the fuel, so that no difference in efficiency is obtained when referring to the dried or as-received lignite and values in line with IGCC plants fed with bituminous coal are obtained (up to 35.15 and 37.12% for the cases with CO_2 capture, depending on the CT technology). Referring to the HHV efficiency values in Tables III and IV, it is possible to appreciate a difference of no less than 7.7 percentage points (for cases A30 and B30), which does not depend on the CT technology. The most significant difference results in 9.1 percentage points for cases A10 and B10.

Different CT technologies clearly affect IGCC performance: efficiency gains up to 2 percentage points and the overall power production increases thanks to higher power output from both the CT expander and the steam turbine. As a matter of fact, when considering technology B, the topping cycle exploits a higher TIT and the bottoming cycle receives more heat from the gasification island. Besides this point, the higher the residual moisture in the lignite, the higher the power output from the steam turbine because of the higher heat related to syngas cooling.

As regards the AGR station, the electric duties are detailed in Table V, where the amine pump consumption

Table III. Main results for the reference IGCC systems without CO_2 capture.

	A10	A20	A30	B10	B20	B30
Cold gas efficiency, %	75.8	73.1	69.7	75.1	72.4	68.9
Net electric power, MW_{el}	798.6	826.0	856.1	920.1	950.9	985.7
Net electric HHV efficiency, %	44.29	43.37	41.77	46.26	45.21	43.47
Net electric $LHV_{a.r.}$ efficiency, %	56.40	55.23	53.19	58.91	57.57	55.35
Net electric $LHV_{a.d.}$ efficiency, %	46.62	46.30	45.40	48.70	48.26	47.25
Specific emissions, kg_{CO2}/MWh	764.2	777.6	804.3	731.1	745.8	772.5

Table IV. Power balances for the investigated IGCC systems with CO_2 capture.

	A10	A20	A30	B10	B20	B30
Referred to one gasification train, MW_{el}						
Combustion turbine	228.4	227.1	225.1	277.6	276.2	274.1
Steam turbine	246.1	270.1	306.2	262.4	289.1	327.9
CT auxiliaries	−0.8	−0.8	−0.8	−1.0	−1.0	−1.0
Heat recovery steam cycle pumps	−5.8	−6.2	−6.8	−6.1	−6.5	−7.1
Coal and ash handling	−5.9	−6.2	−6.7	−6.5	−6.9	−7.4
Vapor compression for coal drying	−21.4	−22.2	−25.0	−23.7	−24.6	−27.7
Air booster compressor	−28.9	−32.3	−37.3	−24.6	−27.5	−31.8
AGR auxiliaries	−3.6	−3.9	−4.2	−3.7	−3.9	−4.3
CO_2 compression	−34.6	−37.0	−40.4	−38.3	−41.0	−44.9
Other IGCC auxiliaries	−2.5	−2.7	−3.0	−2.7	−2.9	−3.2
Overall results						
Cold gas efficiency, %	67.8	65.6	62.6	66.9	64.7	61.7
Thermal input on an HHV basis, MW	2110.7	2223.9	2392.4	2335.5	2464.1	2656.1
Thermal input on an $LHV_{a.r.}$ basis, MW	1657.8	1746.8	1879.1	1834.4	1935.4	2086.2
Thermal input on an $LHV_{a.d.}$ basis, MW	2005.0	2083.4	2200.9	2218.6	2308.4	2443.5
Gross electric power, MW_{el}	949.0	994.5	1062.7	1080.0	1130.6	1203.9
Net electric power, MW_{el}	741.9	772.0	814.5	866.9	902.2	949.1
Net electric HHV efficiency, %	35.15	34.71	34.05	37.12	36.62	35.73
Net electric $LHV_{a.r.}$ efficiency, %	44.76	44.21	43.36	47.27	46.63	45.50
Net electric $LHV_{a.d.}$ efficiency, %	37.00	37.05	37.01	39.08	39.08	38.84
Specific emissions, kg_{CO2}/MWh	104.6	107.1	111.3	98.7	101.5	105.5
CO_2 avoided, %	90.3	90.3	90.3	90.4	90.4	90.4
SPECCA, MJ/kg_{CO2}	3.21	3.09	2.82	3.03	2.90	2.69

is the most significant item, but the overall impact on the IGCC balance is quite limited (Table IV). Figure 6a shows that the required specification for feeding a Claus plant can be satisfied, for case B10, by considering the scheme with a recycle stream and a solvent flow rate up to about 45 kg/s (i.e., an L/G ratio, related to inert flow rates, of 0.31). Similar results can be obtained also for the other considered cases, although not shown here. The optimal flow rate was chosen with the aim of removing enough H_2S to avoid a content in the final CO_2-rich stream exiting the CO_2 removal section higher than 200 ppm(v) on a dry basis. As reported in Figure 6b for case B10, solvent flow rates lower than about 39 kg/s (i.e., an L/G of 0.27) cannot guarantee the desired removal of H_2S, if the scheme with a recycle stream is applied. On the contrary, this specification can be fulfilled for a wider range of flow rates by considering a scheme without recycle, because the amount of H_2S needed to be absorbed is lower. Finally, a solvent flow rate of 40 kg/s (i.e., an L/G of 0.28) was chosen for case B10.[1]

As for the H_2S removal section, the reboiler duty required at the distillation column to regenerate the solvent in the scheme with recycle results higher than the one obtained in the scheme with no recycle (Figure 7), because of the increased acid gas flow rate absorbed and then released in the stripper. In particular, such H_2S flow rate roughly doubles with the recycle. However, because of the lower co-absorption of CO_2, the heat duty of the stripper reboiler increases by less than the double.

The reboiler duty necessary in the CO_2 removal section is very significant if compared with the one required in the H_2S removal section, as reported in Table VI. The two regeneration units differ because of the amount of circulation rate, which is directly related to the conditions of the syngas entering the AGR plant, as CO_2 mass flow rate is orders of magnitude higher than the H_2S one. The highest energy consumption for CO_2 stripping results for case B30, which is the one with the highest amount of CO_2 in the syngas to be purified. As a matter of fact, the higher the amount of CO_2 entering the absorber and the lower the operating pressure (Table II), the higher the amount of required amine solution.

Dealing with decarbonized power production, a measure of the energy cost related to CO_2 capture must be introduced along with IGCC efficiency. Table IV reports the specific primary energy consumption for CO_2 avoided (SPECCA) defined as:

$$\mathrm{SPECCA} = \frac{\mathrm{HR} - \mathrm{HR}_{\mathrm{ref}}}{\mathrm{ER}_{\mathrm{ref}} - \mathrm{ER}} = \frac{3600 \cdot \left(\frac{1}{\eta} - \frac{1}{\eta_{\mathrm{ref}}}\right)}{\mathrm{ER}_{\mathrm{ref}} - \mathrm{ER}} \qquad (2)$$

[1]The circulation rate of all the other analyzed cases was determined on the basis of the same criteria shown for case B10. As a result, a similar L/G ratio (about 0.28) has been obtained for cases B20 and B30, for which the required solvent flow rates are 42 and 43 kg/s, respectively. For cases A10, A20, and A30, 38, 44, and 46 kg/s of amine solutions are needed, with a resulting L/G ratio of about 0.30.

Table V. Breakdown of AGR electric duties (data refer to a single train).

	A10	A20	A30	B10	B20	B30
H_2S removal station, kW_{el}						
Recycle compressor	−267	−312	−325	−248	−256	−260
Amine pump	−81	−92	−95	−69	−72	−73
Heat rejection system	−4	−4	−4	−4	−4	−4
CO_2 removal station, kW_{el}						
Compressor next to the flash unit	−44	−53	−54	−36	−38	−38
Amine pump	−1158	−1238	−1352	−1171	−1259	−1419
Heat rejection system	−252	−270	−294	−317	−341	−385

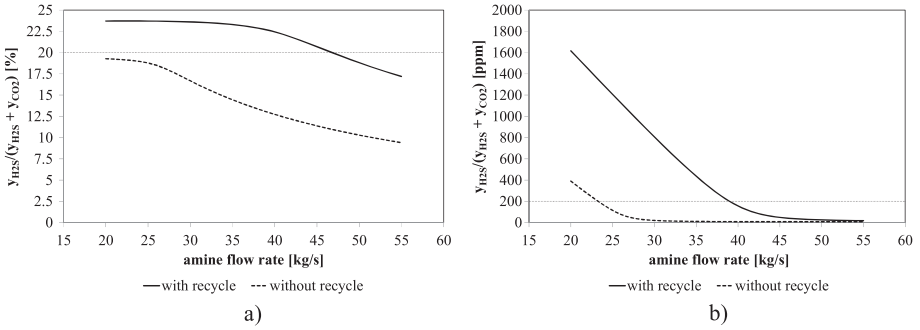

Figure 6. H_2S content (on a dry basis) vs. amine solvent flow rate for case B10: (a) in the stream fed to the Claus plant (the minimum H_2S content in the acid gas is 20 vol.%) and (b) in the CO_2-rich stream to be sent to storage (with the H_2S content limited to less than 200 ppm).

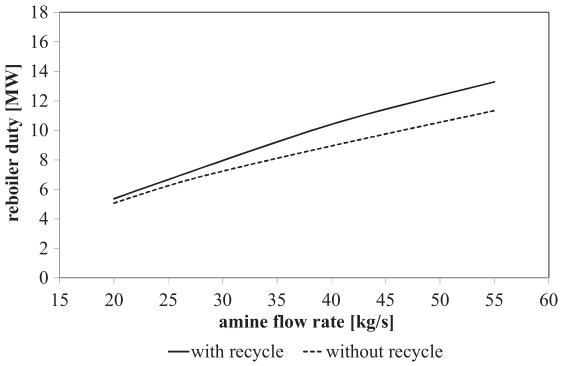

Figure 7. Required reboiler duty vs. amine solvent flow rate for case B10.

where HR is the heat rate (kJ/kWh) of the power plant, ER is the CO_2 emission rate (kg_{CO2}/kWh), and the subscript ref stands for the power plant without CO_2 capture. The reference IGCC system without CO_2 capture, fired with dried lignite with the same residual moisture content, is considered for the calculation of the SPECCA values in Table IV and use of the HHV efficiency is made. On the whole, SPECCA values in Table IV are slightly lower than the ones calculated for IGCC systems fired with a low-sulfur bituminous coal [13]. In particular, when limiting the lignite drying to a residual moisture fixed to 30 wt.%, cases A30 and B30 show the lowest SPECCA values that can be justified by considering the lower efficiency of the corresponding power plant with no CO_2 capture [19]. This trend shows that efficiency penalty associated to CO_2 capture is lower with respect to the corresponding case with no CO_2 capture when lignite with higher residual moisture is gasified, mainly thanks to the lower steam extraction from the bottoming cycle to the WGS station, with less detrimental effects on the steam turbine power output. On the other hand, the higher residual moisture in the lignite leads to increased oxidation air flow rates to the gasifier (Table VI), bringing about larger components in the gasification station as well as a larger size steam turbine, reflecting on the investment costs of the power plant.

With reference to a single gasification train, some details of the main streams numbered in Figure 1 are reported in Table VI. Focusing on a specific CT technology, clear trends can be appreciated for both the mass flow rates and the heat flows to and out of the heat recovery steam cycle. A separate consideration concerns the stoichiometric flame temperature whose value reduces when the residual moisture in the lignite is higher, because of the increased inert N_2 content, brought by the higher oxidation air flow rate in the gasifier. Thus, low NO_x emissions seem to be possible with no need of post-combustion abatement with selective catalytic reduction [61].

Finally, based on the results of the investigated IGCC systems, Figure 8 represents a quick overview of the main IGCC performance, as the specific CO_2 emissions vs. IGCC efficiency. However, some considerations on the performance of IGCC plants with lignite instead of bituminous coal gasification are necessary to better realize the potential of exploiting both air-blown gasification and CO_2 capture technologies. According to previous authors' results [13] and focusing on IGCC

Table VI. Main stream details for one gasification train of the investigated IGCC systems with CO_2 capture.

	A10	A20	A30	B10	B20	B30
Lignite to the drying system, kg/s	116.4	122.7	132.0	128.8	135.9	146.5
Dried coal to gasifier, kg/s	45.3	53.7	66.0	50.1	59.5	73.3
Air at CT compressor inlet, kg/s	683.8	687.2	692.2	686.4	690.2	696.0
Air to the gasification system, kg/s	137.9	154.4	178.8	155.2	173.9	201.9
Coal-derived gas exiting the gasifier, kg/s	194.2	221.2	261.1	217.4	247.9	293.2
Gasifier pressure, bar	37.0	37.0	37.0	30.4	30.4	30.4
MP steam to the WGS station, kg/s	42.5	35.5	25.4	45.6	37.6	26.1
Fuel gas to CT combustor, kg/s	119.1	132.2	151.6	133.8	148.7	170.9
Fuel gas LHV, MJ/kg	5.71	5.17	4.55	5.55	5.02	4.41
Stoichiometric flame temperature, K	2151.0	2100.1	2031.1	2130.8	2078.8	2008.2
Gas temperature at CT outlet, °C	585.0	585.1	585.2	596.8	596.9	597.0
Heat recovered in HRSG, MW	341.5	344.1	347.6	352.2	354.6	357.5
HT syngas cooling, MW	327.3	365.9	423.6	360.4	403.4	468.1
Heat from gasifier membrane walls, MW	20.1	20.8	22.0	22.2	23.1	24.4
HP steam entering the turbine,* kg/s	396.1	418.3	451.5	421.3	445.5	480.0
Heat rejected at the condenser,* MW	268.5	298.3	343.0	271.3	304.3	352.6
Heat for H_2S stripping, MW	9.9	11.1	11.7	10.4	10.9	11.1
Heat for CO_2 stripping, MW	107.4	114.6	125.3	128.7	138.0	153.9

*Overall result that accounts for two gasification trains

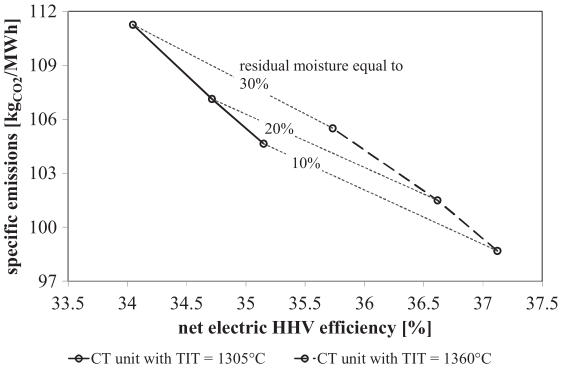

Figure 8. Specific CO_2 emissions vs. HHV efficiency for the IGCC systems investigated in the work, depending on the residual moisture in the lignite after drying.

systems with the advanced CT unit for the sake of technological prospects, air-blown gasification of lignite brings about a reduction in HHV efficiency equal to almost 1.5 to 2.8 percentage points, depending on the residual moisture in the dried lignite. The lower the residual moisture in lignite after drying, the minimum the efficiency reduction, considering that the moisture content in the bituminous coal used as fuel input in former calculations [13] was 8%, that is, similar to the one in case B10. Thus, the HHV efficiency reduction, calculated almost equal to 1.5 percentage points, may be considered as the energy cost mainly due to of the significant lignite drying.

5. CONCLUSIONS

An original study focusing on air-blown IGCC systems fired with dried lignite and including pre-combustion CO_2 capture has been proposed. In particular, two CT technologies have been considered for the topping cycle: a proven machine and an advanced one, with lower and higher TIT, respectively. For both the technologies, attention to the calculations of the AGR units has been paid as well. In particular, the operation of the H_2S removal section, with a limited impact on the IGCC power balances, is questionable because of the very low amount of sulfur in the raw lignite, and a particular technique was adopted to fulfill the requirements related to the presence of H_2S in the stream to the Claus plant and in the CO_2-rich stream to storage.

Two main figures of merit have been considered and discussed to evaluate the potential of the investigated IGCC systems: the HHV efficiency and the SPECCA. On one side, a significant decrease in HHV efficiency is accomplished when gasifying dried lignite with higher residual moisture: HHV efficiency differences with respect to the reference case with no CO_2 capture range from 7.7 to 9.1 percentage points.

On the other side, when firing the IGCC systems with and without CO_2 capture with the same dried lignite, SPECCA reductions are possible in case of dried lignite with higher residual moisture, with a value as low as 2.69 MJ/kg_{CO2}.

Ultimately, based on a previous authors' study on similar IGCC systems [13] where a more common bituminous coal was used as fuel input, air-blown gasification of lignite in power plants with the advanced CT brings about a reduction in HHV efficiency equal to almost 1.5 to 2.8 percentage points, depending on the residual moisture in the dried lignite.

NOMENCLATURE

AGR	= acid gas removal
a.d.	= after drying
a.r.	= as received

CCS	= carbon capture and storage
CGE	= cold gas efficiency
CT	= combustion turbine
d.b.	= dry basis
G	= mass flow rate, kg/s
HHV, LHV	= higher, lower heating value, MJ/kg
HP, MP	= high, medium pressure
HRSG	= heat recovery steam generator
HT, LT	= high, low temperature
IGCC	= integrated gasification combined cycle
L/G	= liquid-to-gas ratio
MDEA	= methyldiethanolamine
MHI	= Mitsubishi Heavy Industries
NRTL	= non-random two-liquid
PR	= Peng–Robinson
R&D	= research and development
SCOT	= Shell Claus off-gas treatment
SPECCA	= specific primary energy consumption for CO_2 avoided, MJ/kg_{CO2}
TIT	= turbine inlet temperature, °C
y	= mole fraction in vapor phase
WGS	= water–gas shift
WTA	= Wirbelschicht Trocknung mit interner Abwärmenutzung
η	= efficiency

APPENDIX A:

This paragraph reports the main assumptions for the IGCC system components as simulated in this work.

Table A.1. Main assumptions for gasification station calculations.

	A	B
Gasification pressure, bar	37	30.4
Combustor/reductor temperature, °C	1900/1200	
Carbon conversion, %	99.9	
Heat to membrane walls, % of dried lignite thermal input	2	
Temperature/pressure of gasifying air, °C/bar	541/43.5	495/35.8
Air booster polytropic efficiency, %	90.5	
Heat loss in syngas coolers, % of transferred heat	0.7	
Pressure loss in syngas coolers, %	2	
Steam-to-CO ratio at first WGS reactor	1.5	
Pressure loss in WGS reactors, %	3	
Syngas temperature at second WGS inlet, °C	210	

Table A.2. Main assumptions for CT performance simulation.

	A	B
Air filter pressure loss, %	1	
Compressor pressure ratio	18.1	
Compressor polytropic efficiency, %	90.5	92.5
Compressor leakage, % of the inlet flow	0.75	
Air pressure loss, %	4	3
Cooled turbine stage isentropic efficiency, %	88	91.15
Uncooled turbine stage isentropic efficiency, %	90	92.15
Turbine inlet temperature, °C	1305	1360
Fuel valve pressure loss, bar	10	5
Mass flow rate at CT outlet, kg/s	665	
Turbine/compressor mechanical efficiency, %	99.865	
CT auxiliaries, % of gross power	0.35	
Electric generator efficiency, %	98.7	

Table A.3. Main characteristics of the H_2S and of the CO_2 removal simulation.

	H_2S	CO_2
Number of trains	2	2
Number of absorption columns per train	1	2
Absorber real trays	12	51
MDEA concentration in the aqueous solution, wt.%	10	50
Lean solution CO_2 loading	0.03	0.02
Rich solution CO_2 loading	0.90	0.76
Number of regeneration columns per train	1	1
Reboiler pressure, bar	1.1	1.1
Regeneration column real trays	13	8
Minimum ΔT in the recuperative heat exchanger	10	5

REFERENCES

1. Grammelis P, Kakaras E, Koukouzas N. The perspectives of energy production from coal-fired power plants in an enlarged EU. *International Journal of Energy Research* 2004; **28**:799–815.
2. Shen CH, Chen WH, Hsu HW, Sheu JY, Hsieh TH. Co-gasification performance of coal and petroleum coke blends in a pilot-scale pressurized entrained-flow gasifier. *International Journal of Energy Research* 2012; **36**:499–508.
3. Shim HM, Chun WG, Kim HT. Comparative simulation of hydrogen production derived from gasification system with CO2 reduction by various feedstocks. *International Journal of Energy Research* 2010; **34**: 412–421.
4. Long HA, Wang T. A system performance and economics analysis of IGCC with supercritical steam bottom cycle supplied with varying blends of coal and biomass feedstock. *International Journal of Energy Research* 2014; **38**:189–204.

5. Hashimoto T, Ota K, Fujii T. Progress update for commercial plants of air blown IGCC. *Proceedings of ASME Turbo Expo* 2007; **1**:499–504. doi:10.1115/GT2007-28348.
6. Hashimoto T, Sakamoto K, Yamaguchi Y, Oura K, Arima K, Suzuki T. Overview of integrated coal gasification combined-cycle technology using low-rank coal. *Mitsubishi Heavy Industries Technical Review* 2011; **48**(3):19–23.
7. Giuffrida A, Romano MC, Lozza G. Thermodynamic analysis of air-blown gasification for IGCC applications. *Applied Energy* 2011; **88**(11):3949–3958. doi:10.1016/j.apenergy.2011.04.009.
8. Ishibashi Y, Shinada O. First year operation results of CCP's Nakoso 250 MW air-blown IGCC demonstration plant. Gasification Technologies Conference 2008, Washington, DC, USA
9. Giuffrida A, Romano MC, Lozza G. Efficiency enhancement in IGCC power plants with air-blown gasification and hot gas clean-up. *Energy* 2013; **53**:221–229. doi:10.1016/j.energy.2013.02.007.
10. Giuffrida A, Romano MC, Lozza G. CO_2 capture from air-blown gasification-based combined cycles. *Proceedings of ASME Turbo Expo* 2012; **3**:395–404. doi:10.1115/GT2012-69787.
11. Giuffrida A, Bonalumi D, Lozza G. Amine-based post-combustion CO_2 capture in air-blown IGCC systems with cold and hot gas clean-up. *Applied Energy* 2013; **110**:44–54. doi:10.1016/j.apenergy.2013.04.032.
12. Bonalumi D, Giuffrida A, Lozza G. A study of CO_2 capture in advanced IGCC systems by ammonia scrubbing. *Energy Procedia* 2014; **45**:663–670. doi:10.1016/j.egypro.2014.01.071.
13. Moioli S, Giuffrida A, Gamba S, Romano MC, Pellegrini L, Lozza G. Pre-combustion CO_2 capture by MDEA process in IGCC based on air-blown gasification. *Energy Procedia* 2014; **63**:2045–2053. doi:10.1016/J.EGYPRO.2014.11.220.
14. Klimantos P, Koukouzas N, Kakaras E, Typou I. Pre-combustion CO_2 capture in low rank coal gasification combined cycle power plants. Proceedings of the 8th International Conference on Greenhouse Gas Control Technologies (GHGT-8), June 19−22, 2006, Trondheim, Norway
15. Gräbner M, Von Morstein O, Rappold D, Günster W, Beysel G, Meyer B. Constructability study on a German reference IGCC power plant with and without CO_2 capture for hard coal and lignite. *Energy Conversion and Management* 2010; **51**:2179–2187. doi:10.1016/j.enconman.2010.03.011.
16. NETL. Cost and performance baseline for fossil energy plants. Volume 3a: Low rank coal to electricity: IGCC cases. Report DOE/NETL-2010/1399, May 2011 - Available from: www.netl.doe.gov/File%20-Library/Research/Energy%20Analysis/Publications/LR_IGCC_FR_20110511.pdf
17. Mondol JD, McIlveen-Wright D, Rezvani S, Huang Y, Hewitt N. Techno-economic evaluation of advanced IGCC lignite coal fuelled power plants with CO_2 capture. *Fuel* 2009; **88**:2495–2506. doi:10.1016/j.fuel.2009.04.019.
18. Maas P, Scherer V. Lignite fired IGCC with ceramic membranes for CO_2 separation. *Energy Procedia* 2014; **63**:1976–1985. doi:10.1016/J.EGYPRO.2014.11.212.
19. Giuffrida A. Impact of low-rank coal on air-blown IGCC performance. *Proceedings of ASME Turbo Expo* 2014; **3A**. doi:10.1115/GT2014-26843.
20. Kakaras E, Ahladas P, Syrmopoulos S. Computer simulation studies for the integration of an external dryer into a Greek lignite-fired power plant. *Fuel* 2002; **81**(5):583–593.
21. EBTF. European best practice guidelines for assessment of CO_2 capture technologies. February 2011 - Available from: http://www.energia.polimi.it/news/D%204_9%20best%20practice%20guide.pdf
22. Moioli S, Pellegrini LA. Regeneration section of CO_2 capture plant by MEA scrubbing with a rate-based model. *Chemical Engineering Transactions* 2013; **32**:1849–1854.
23. Langé S, Moioli S, Pellegrini LA. Vapor–liquid equilibrium and enthalpy of absorption of the CO_2–MEA–H_2O system. *Chemical Engineering Transactions* 2015; **43**:1975–1980.
24. Salkuyeh YK, Mofarahi M. Reduction of CO_2 capture plant energy requirement by selecting a suitable solvent and analyzing the operating parameters. *International Journal of Energy Research* 2013; **37**(8):973–981.
25. http://www.gecos.polimi.it/software/gs.php
26. Chiesa P, Macchi E. A thermodynamic analysis of different options to break 60% electric efficiency in combined cycle power plants. *Journal of Engineering for Gas Turbine and Power* 2004; **126**(4):770–785. doi:10.1115/1.1771684.
27. Giuffrida A, Romano MC. On the effects of syngas clean-up temperature in IGCCs. *Proceedings of ASME Turbo Expo* 2010; **3**:661–670. doi:10.1115/GT2010-22752.
28. Giuffrida A, Romano MC, Lozza G. Thermodynamic assessment of IGCC power plants with hot fuel gas desulfurization. *Applied Energy* 2010; **87**(11):3374–3383. doi:10.1016/j.apenergy.2010.05.020.
29. Li CZ. *Advances in the Science of Victorian Brown Coal*. Elsevier: Oxford, UK, 2004. ISBN:978-0-08-044269-3.
30. De Guido G, Langè S, Moioli S, Pellegrini LA. Thermodynamic method for the prediction of solid CO_2

formation from multicomponent mixtures. *Process Safety and Environmental Protection* 2014; **92**:70–79.
31. Chen CC, Britt HI, Boston JF, Evans LB. Extension and application of the Pitzer equation for vapor–liquid equilibrium of aqueous electrolyte systems with molecular solutes. *AIChE Journal* 1979; **25**:820–831.
32. Chen CC, Britt HI, Boston JF, Evans LB. Local composition model for excess Gibbs energy of electrolyte systems. Part I: single solvent, single completely dissociated electrolyte systems. *AIChE Journal* 1982; **28**:588–596.
33. Mock B, Evans LB, Chen CC. Thermodynamic representation of phase equilibria of mixed-solvent electrolyte systems. *AIChE Journal* 1986; **32**(10): 1655–1664.
34. Chen CC, Evans LB. A local composition model for the excess Gibbs energy of aqueous electrolyte systems. *AIChE Journal* 1986; **32**:444–454.
35. Langé S, Pellegrini LA, Moioli S, Picutti B, Vergani P. Influence of gas impurities on thermodynamics of amine solutions. 1. Aromatics. *Industrial & Engineering Chemistry Research* 2013; **52**(5):2018–2024.
36. Pellegrini LA, Langé S, Moioli S, Picutti B, Vergani P. Influence of gas impurities on thermodynamics of amine solutions. 2. Mercaptans. *Industrial & Engineering Chemistry Research* 2013; **52**(5):2025–2031.
37. Lewis WK, Whitman WG. Principles of gas absorption. *Industrial and Engineering Chemistry* 1924; **16**(12): 1215–1220.
38. Astarita G, Savage DW, Bisio A. *Gas Treating with Chemical Solvents*. Wiley: New York, 1983.
39. Fu K, Chen G, Liang Z, Sema T, Idem R, Tontiwachwuthikul P. Analysis of mass transfer performance of monoethanolamine-based CO2 absorption in a packed column using artificial neural networks. *Industrial & Engineering Chemistry Research* 2014; **53**:4413–4423.
40. Choi SY, Nam SC, Yoon YI, Park KT, Park S-J. Carbon dioxide absorption into aqueous blends of methyldiethanolamine (MDEA) and alkyl amines containing multiple amino groups. *Industrial & Engineering Chemistry Research* 2014; **53**:14451–14461.
41. Park HM. Reduced-order modeling of carbon dioxide absorption and desorption with potassium carbonate promoted by piperazine. *International Journal of Heat and Mass Transfer* 2014; **73**:600–615.
42. Cullinane JT, Rochelle GT. Kinetics of carbon dioxide absorption into aqueous potassium carbonate and piperazine. *Industrial & Engineering Chemistry Research* 2005; **45**:2531–2545.
43. Freguia S. *Modeling of CO_2 Removal from Flue Gase with Monoethanolamine*. [M.S.E. Thesis]. The University of Texas: Austin, Texas, 2002.
44. Chen X. Carbon dioxide thermodynamics, kinetics, and mass transfer in aqueous piperazine derivatives and other amines [PhD thesis]. The University of Texas: Austin, Texas, USA, 2011.
45. Prasher BD, Fricke AL. Mass transfer at a free gas–liquid interface in turbulent thin films. *Industrial & Engineering Chemistry Process Design and Development* 1974; **13**:336–340.
46. Cullinane JT. Thermodynamics and kinetics of aqueous piperazine with potassium carbonate for carbon dioxide absorption [PhD Thesis]. The University of Texas, Austin, Texas, USA, 2005.
47. King CJ. Turbulent liquid phase mass transfer at a free gas–liquid interface. *Industrial and Engineering Chemistry Fundamentals* 1966; **5**(1):1–8.
48. Moioli S, Pellegrini LA, Picutti B, Vergani P. Improved rate-based modeling of H_2S and CO_2 removal by MDEA scrubbing. *Industrial & Engineering Chemistry Research* 2013; **52**(5):2056–2065.
49. Moioli S, Pellegrini LA. Improved rate-based modeling of the process of CO_2 capture with PZ solution. *Chemical Engineering Research and Design* 2015; **93**:611–620. doi:10.1016/j.cherd.2014.03.022.
50. Moioli S, Pellegrini LA. Physical properties of PZ solution used as a solvent for CO_2 removal. *Chemical Engineering Research and Design* 2015; **93**:720–726. doi:10.1016/j.cherd.2014.06.016.
51. Naami A, Edali M, Sema T, Idem R, Tontiwachwuthikul P. Mass transfer performance of CO_2 absorption into aqueous solutions of 4-diethylamino-2-butanol, monoethanolamine, and N-methyldiethanolamine. *Industrial & Engineering Chemistry Research* 2012; **51**:6470–6479.
52. Daviet GR, Donnelly ST, Bullin JA. *Dome's North Caroline Plant Succesful Conversion to MDEA*. Sixty-Third GPA Annual Convention. Gas Processor Association: Tulsa, OK, 1984; 75–79.
53. Pellegrini LA, Moioli S, Munari FM, Vergani P, Picutti B, Uccelletti A. The acid Gas removal unit at GASCO'S Habshan 5: simulation and comparison with field data. 12th Offshore Mediterranean Conference and Exhibition OMC2015. Ravenna, Italy, 2015.
54. Kidnay AJ, Parrish WR. *Fundamentals of Natural Gas Processing*. Taylor & Francis Group: Boca Raton, FL, USA, 2006.
55. Kohl AL, Nielsen R. *Gas Purification*. Gulf Publishing Company, Book Division: Houston, TX, USA, 1997.
56. Rho SW, Yoo KP, Lee JS, Nam SC, Son JE, Min BM. Solubility of CO_2 in aqueous methyldiethanolamine solutions. *Journal of Chemical & Engineering Data* 1997; **42**(6):1161–1164.

57. Lunsford KM, Bullin JA. *Optimization of Amine Sweetening Units. AIChE Spring National Meeting*. American Institute of Chemical Engineers: New York, 1996.
58. Guo XP, Tomoe Y. The effect of corrosion product layers on the anodic and cathodic reactions of carbon steel in CO_2-saturated mdea solutions at 100°C. *Corrosion Science* 1999; **41**:1391–1402.
59. Xu GW, Zhang CF, Qin SJ, Gao WH, Liu HB. Gas–liquid equilibrium in a CO_2–MDEA–H_2O system and the effect of piperazine on it. *Industrial & Engineering Chemistry Research* 1998; **37**:1473–1477.
60. Adams TA, Barton PI. High-efficiency power production from coal with carbon capture. *AIChE Journal* 2010; **56**(12):3120–3136.
61. Chiesa P, Lozza G, Mazzocchi L. Using hydrogen as gas turbine fuel. *Journal of Engineering for Gas Turbine and Power* 2005; **127**(1):73–80. doi:10.1115/1.1787513.